ACS APPLIED MATERIALS & INTERFACES

Research Article

www.acsami.org

"Plug and Play" Logic Gates Based on Fluorescence Switching Regulated by Self-Assembly of Nucleotide and Lanthanide Ions

Fang Pu,[†] Jinsong Ren,*[,†] and Xiaogang Qu*[,†]

[†]Laboratory of Chemical Biology and State Key laboratory of Rare Earth Resources Utilization, Changchun Institute of Applied Chemistry, Chinese Academy of Sciences, Changchun 130022, People's Republic of China

Supporting Information

ABSTRACT: Molecular logic gates in response to chemical, biological, or optical input signals at a molecular level have received much interest over the past decade. Herein, we construct "plug and play" logic systems based on the fluorescence switching of guest molecules confined in coordination polymer nanoparticles generated from nucleotide and lanthanide ions. In the system, the addition of new modules directly enables new logic functions. PASS 0, YES, PASS 1, NOT, IMP, OR, and AND gates are successfully constructed in sequence. Moreover, different logic gates (AND, INH, and IMP) can be constructed using different guest molecules and the same input combinations. The work will be beneficial to the future logic design and expand the applications of coordination polymers.

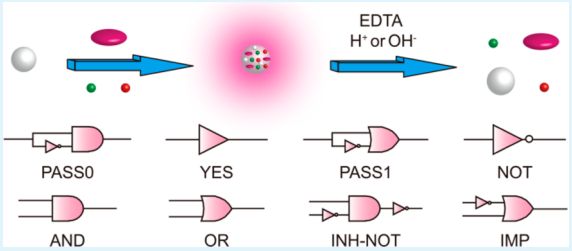

KEYWORDS: *plug and play, logic gate, coordination polymer, fluorescence switching, nucleotide*

INTRODUCTION

Since the inception of the first molecular logic gate by de Silva et al.,[1] many types of logic gates responsive to physical and/or chemical signals have been successfully demonstrated as an alternative to traditional silicon-based information processing systems.[2−7] For basic molecular logic gates, each design was individual and performed different logic functions in response to different input signals. By employing multiple input combinations, designing complicated organic molecules, or coupling modular computing elements, much larger networking systems could be constructed.[8,9] Besides, fuzzy logic and multivalued logic systems have also been explored as a superset of Boolean logic system.[10,11] Recently, de Silva et al. fabricated a "plug and play" molecular logic system by arranging the association between easily available lumophores and receptors in detergent micelles.[12] In the design of "plug and play" system, the addition of new modules directly enabled new logic functions and gave rise to a set of logic gates serially. That is, the molecular logic type could be altered simply by adding another component, which increases the flexibility of molecular logic designs. It is different from previous reconfigurable logic gates, which were constructed only by changing the input molecules or redesigning the gate.[13] Thus, the design further pushed the conceptual development of molecular computing. However, regardless of the only example, no reliable "plug and play" logic gate has been achieved so far.

Up to now, a variety of molecules and materials were used for the construction of molecular logic gates. Among them, nucleic acids as building blocks have received increasing attention due to their unique chemical, biological, and structural properties.[14−23] Nucleotides are biological molecules that form the building blocks of nucleic acids (DNA and RNA) and play central roles in living organisms.[24] Moreover, nucleotides are very attractive ligands as they contain multiple high affinity metal binding sites and chirality. These properties have shed exciting light on the self-assembly or biomimetic synthesis of functional nanomaterials using nucleotides as templates.[25−37] However, limited attention has been paid to the materials for constructing logic gates until now. Akkaya and co-worker constructed a NAND gate based on Watson−Crick base pairing of dAMP and dTMP, and fluorescence change of a DNA-binding dye DAPI.[38] Lanthanides have been employed to construct logic gates due to their optical properties and coordination ability.[39−41] Very recently, we combined the properties of nucleotides, lanthanide ions and guest molecule to integrate logic gates into the intracellular imaging probe.[42] In the present work, we sought to obtain fluorescence switching in a coordination polymer nanoparticle (CPN) system generated from self-assembly of nucleotides and lanthanide ions, thus enabling "plug and play" logic-gate operation. The addition of new modules directly enabled new logic functions. Furthermore, by changing the dyes confined in the CPNs, different logic operations could be achieved. The advantages of simple design, convenient operation, and diverse outputs will be highly useful in future logic system fabrication. The applications of coordination polymers will be further extended.

EXPERIMENTAL SECTION

Materials. Guanosine 5′-monophosphate (GMP) and Na_2EDTA were purchased from Sigma-Aldrich. N-Methylmesoporphyrin IX

Received: March 31, 2014
Accepted: May 16, 2014
Published: May 16, 2014

   dx.doi.org/10.1021/am501949t | ACS Appl. Mater. Interfaces 2014, 6, 9557−9562

(NMM) was purchased from Porphyrin Products Inc. (Logan, UT), and its concentration was measured by absorbance at 379 nm assuming an extinction coefficient of 1.45×10^5 M^{-1} cm^{-1}. Hoechst 33342 (Hoe) was purchased from Sigma-Aldrich and used without further purification. The extinction coefficient of Hoe is 45 000 M^{-1} cm^{-1} at 350 nm. Fluorescein was obtained from Alfa Aesar. Terbium nitrate hexahydrate ($Tb(NO_3)_3{\cdot}6H_2O$) and europium nitrate hexahydrate ($Eu(NO_3)_3{\cdot}6H_2O$) were purchased from Aladdin Reagent (Shanghai, China). All other reagents were all of analytical reagent grade and used as received.

Methods. Fluorescence spectra were measured on a JASCO FP-6500 spectrophotometer. UV/vis absorption spectra were recorded on a JASCO V-550 spectrophotometer. Scanning electron microscopy (SEM) was conducted on an S-4800 field emission scanning microscope. Transmission electron microscopy (TEM) was conducted on a JEOL JEM-1011 (acceleration voltage, 100 kV).

Preparation of coordination polymer nanoparticles and fluorescence measurement. $Tb(NO_3)_3$ or $Eu(NO_3)_3$ aqueous solutions (5 mM) was added to GMP solution (20 mM) containing NMM (20 μM) under slight shaking. Solid products of GMP/NMM/lanthanide ions were formed immediately. The products were kept at room temperature for 30 min. Ten microliters of the complex was drawn out and diluted with 400 μL of H_2O. Then the fluorescence spectra were measured with the excitation wavelength of 399 nm. The CPNs containing other dyes were prepared in the same way. The excitation wavelengths were 485 and 352 nm for CPNs containing Flu and Hoe, respectively.

RESULTS AND DISCUSSION

In the experiments, the coordination polymer nanoparticles were formed immediately upon mixing guanosine 5′-monophosphate (GMP) and lanthanide ions (Eu^{3+} or Tb^{3+}) at room temperature in aqueous solution. The products GMP/Eu^{3+} and GMP/Tb^{3+} appeared irregular spheres with an average diameter of 30 and 22 nm, respectively (Figure S1A,B, Supporting Information). Phosphate group and nucleobase moiety of GMP were involved in the coordination with lanthanide ions.[42] N-methylmesoporphyrin IX (NMM) is a commercially available unsymmetrical anionic porphyrin, whose structure is shown in Scheme 1. It is weakly fluorescent in aqueous solution. The fluorescence enhancement of NMM was realized by mixing GMP, NMM, and lanthanide ions together. As shown in Figure 1, the complexes GMP/NMM/Tb^{3+} and GMP/NMM/Eu^{3+} emitted strong red fluorescence with a peak centered at 612 nm upon excitation with a 399 nm light. The introduction of NMM into the coordination networks did not affect the morphology of nanoparticles, as confirmed by SEM and TEM observation (Figure S1C,D, Figure S2, Supporting Information). It indicates the key feature of adaptive inclusion of host assemblies. The self-assembly of the ternary complex could be easily tuned by external stimuli such as pH and EDTA.[42] After addition of HCl, NaOH, or EDTA, a disassembly occurred within 1 min. NMM was released and dispersed into the solution. Nearly no fluorescence at 612 nm was observed (Figure 1). These features would provide potential opportunities for the smart material as logic gates.

First, GMP served as a gate and the Tb^{3+} ion was defined as input 1. The relative fluorescence intensity of NMM at 612 nm could be regarded as the output with a threshold value of 0.4. The output value was defined as 0 when the relative fluorescence intensity at 612 nm was lower than 0.4, whereas the output value was defined as 1 when the relative intensity was higher than 0.4. Addition of Tb^{3+} to the solution containing GMP alone produced coordination polymer nanoparticles immediately. However, no emission at 612 nm was observed due to the lack of NMM. The result corresponded to the truth table of PASS 0 logic gate, the simplest Boolean logic operation (Figure 2, No. 1,2, Figure S3, Supporting Information). The output signal always is 0 whether the input is 0 or 1. Subsequently, NMM was added to the GMP solution and GMP/NMM acted as a gate. In the presence of NMM, the

Scheme 1. Schematic Illustration of "Plug and Play" Logic Gates Based on Fluorescence Switching Regulated by Self-Assembly of 5′-GMP and Lanthanide Ions[a]

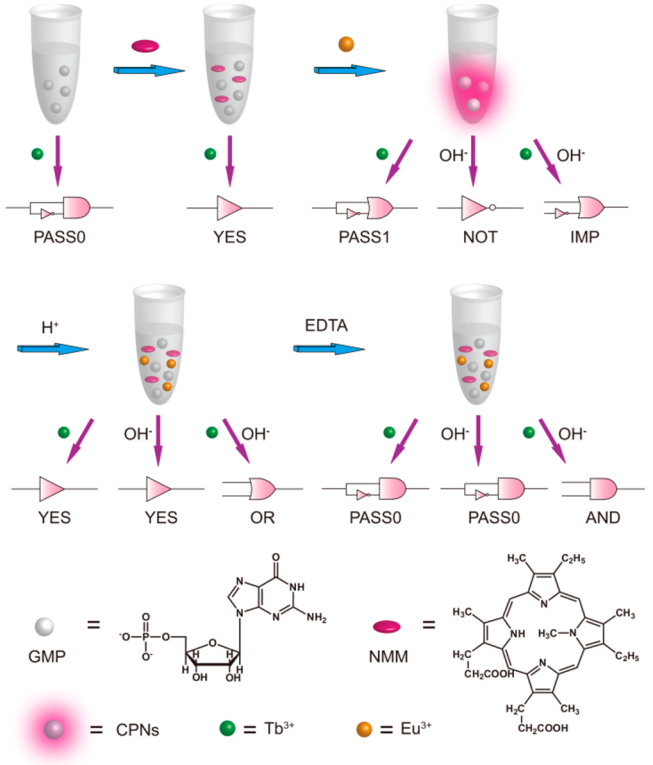

[a]NMM was confined in the adaptive supramolecular networks and showed intense luminescence. After addition of HCl, NaOH, or EDTA, a disassembly of CPNs occurred and fluorescence intensity of NMM decreased. The properties were used to construct versatile logic gates. The chemical structure of GMP and NMM are shown.

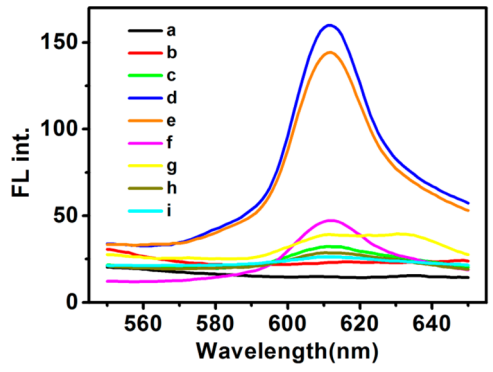

Figure 1. Fluorescence spectra of NMM in different conditions. The excitation wavelength was 399 nm. [GMP] = 0.5 mM, [lanthanide ions] = 0.125 mM, [NMM] = 0.5 μM. (a) GMP alone, (b) GMP/Tb^{3+}, (c) GMP/NMM, (d) GMP/NMM/Tb^{3+}, (e) GMP/NMM/Eu^{3+}, (f) GMP/NMM/Eu^{3+}/H^+, (g) GMP/NMM/Eu^{3+}/OH^-, (h) GMP/NMM/Eu^{3+}/EDTA, and (i) NMM. The GMP/NMM/Tb^{3+} and GMP/NMM/Eu^{3+} CPNs emitted strong fluorescence with a peak centered at 612 nm.

dx.doi.org/10.1021/am501949t | ACS Appl. Mater. Interfaces 2014, 6, 9557−9562

A

System	No	Input1 (Tb^{3+})	Input2 (OH^-)	Output λem = 612 nm	Logic gate
GMP	1	0	-	0	PASS0
	2	1	-	0	
GMP+NMM	3	0	-	0	YES
	4	1	-	1	
GMP+NMM +Eu^{3+}	5	0	-	1	PASS1
	6	1	-	1	
	7	-	0	1	NOT
	8	-	1	0	
	9	0	0	1	IMP
	10	1	0	1	
	11	0	1	0	
	12	1	1	1	
GMP+NMM +Eu^{3+}+H^+	13	0	-	0	YES
	14	1	-	1	
	15	-	0	0	YES
	16	-	1	1	
	17	0	0	0	OR
	18	1	0	1	
	19	0	1	1	
	20	1	1	1	
GMP+NMM +Eu^{3+}+H^+ +EDTA	21	0	-	0	PASS0
	22	1	-	0	
	23	-	0	0	PASS0
	24	-	1	0	
	25	0	0	0	AND
	26	1	0	0	
	27	0	1	0	
	28	1	1	1	

B

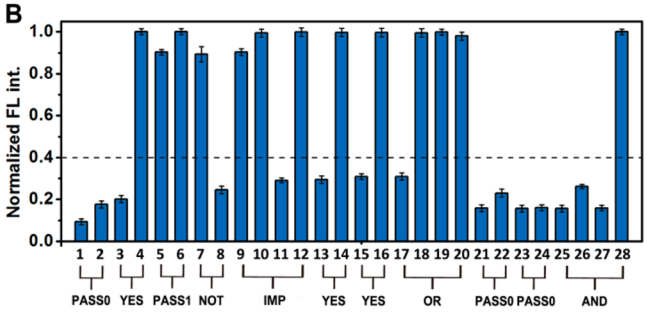

Figure 2. (A) Truth tables for a set of logic gates with the addition of new modules into the gate. (B) Normalized fluorescence intensities of NMM in response to different combinations of the inputs monitored at 612 nm when excited at 399 nm, corresponding to different logic gates.

CPNs generated from GMP and Tb^{3+} emitted a strong light at 612 nm. A YES logic gate, whose output signal is the same as the input signal, was produced (Figure. 2, No. 3,4).

Then a complex of GMP/NMM/Eu^{3+} could be regarded as a gate. NMM exhibited an enhancement in its fluorescence upon encapsulation in CPNs consisting of GMP and Eu^{3+}. Since GMP had interacted with Eu^{3+}, addition of Tb^{3+} to the CPNs of GMP/NMM/Eu^{3+} resulted in little change of the fluorescence intensity, corresponding to a PASS 1 logic gate (Figure 2, No. 5,6). PASS 1 always gives rise to logic value 1 and is independent of the absence or presence of an input. An NOT logic gate, which is the inverse YES gate, requires the output to be opposite to the input. It could be accomplished by using OH^- as input 2 since the fluorescence of NMM confined in CPNs was strong dependent on pH values. As shown in Figure 1, when the pH value of solution containing CPNs was increased to 9.0, the fluorescence intensity was found to be decreased significantly. That is, the addition of OH^- corresponded to an input value of 1, which resulted in an output of 0 (Figure 2, No. 7,8). The four single-output Boolean logic operations (PASS 0, YES, PASS 0, NOT) given above were driven by single-input. To be a more useful system, a logic gate should be multiple-configurable (more than one input). In the case of the double-input, more complex logic gates could be produced. For GMP/NMM/Eu^{3+} system, double-input Tb^{3+} and OH^- could generate an IMPLICATION (IMP) gate, the integration of an OR and a NOT gate (Figure 2, No. 9−12). Although GMP/NMM/Eu^{3+} CPNs would disassemble upon addition of OH^-, the effect of OH^- could be negated by simultaneous addition of Tb^{3+}. It is attributed to the interaction between OH^- and Tb^{3+} and the formation of $Tb(OH)_3$. Thus, the emission of NMM maintained unchanged and the output was 1 when both Tb^{3+} and OH^- were added.

Next, H^+ was introduced to the mixture of GMP/NMM/Eu^{3+} to produce another gate. The formation of CPNs was based on coordination bonds between lanthanide ions and GMP.[42] The disruption of coordination bonds resulted in disassociation of CPNs and subsequent release of NMM into the aqueous solution. The CPNs were sensitive to acidity because protons and lanthanide ions competed to combine with GMP, leading to the physical destabilization of CPNs.[43,44] As shown in Figure S4 (Supporting Information), GMP/NMM/Tb^{3+} CPNs presented intense fluorescence at pH 7.4 and the fluorescence intensities increased slightly with increasing Tb^{3+} concentration. At pH 5.0, CPNs with low concentrations of Tb^{3+} ions disassociated and NMM escaped into the surrounding environment, leading to weak fluorescence. However, in the presence of high concentrations of Tb^{3+}, the CPNs did not disassociate and release NMM. At lower pH, CPNs were unstable and slight fluorescence enhancement occurred in the presence of high concentration of Tb^{3+}. These results suggested the formation and disassociation of CPNs could be regulated by lanthanide ions and H^+ and depended on their concentrations. To perform logic operation, GMP/NMM/Eu^{3+}/H^+ (pH = 5.0) system was employed. Without any input, GMP/NMM/Eu^{3+}/H^+ manifested a low fluorescence signal at 612 nm due to the cleavage of coordination bonds and release of NMM. The single-input Tb^{3+} could negate the effect of H^+ to drive a YES logic gate (Figure 2, No. 13,14), resulting from that excess lanthanide ions could shift the equilibrium to the formation of CPNs. In the case of single-input OH^-, the fluorescence intensity was recovered and a YES logic gate was obtained due to the neutralization of OH^- and H^+ (Figure 2, No. 15,16). For system of GMP/NMM/Eu^{3+}/H^+, an OR gate could be fabricated in the presence of double-input Tb^{3+} and OH^-, in which the output of the gate is 1 if either input is 1 (Figure 2, No. 17−20).

Furthermore, chelator EDTA, which could remove lanthanide ions from the CPNs, was introduced to form a GMP/NMM/Eu^{3+}/H^+/EDTA system as a gate. Without any input, the mixture presented no emission at 612 nm due to the effect of H^+ and EDTA. In the case of single-input Tb^{3+} or OH^-, PASS 0 gate was obtained (Figure 2, No. 21−24). Although Tb^{3+} could negate the effect of EDTA, the fluorescence intensity was still low due to the presence of H^+. The same case happened to H^+ alone, which merely neutralized OH^-. Only adding Tb^{3+} and OH^- simultaneously to negate the effect of EDTA and H^+, an AND logic operation was implemented (Figure 2, No. 25−28).

From what has been discussed above, we demonstrated that more logic operations became accessible from a small set of components. Besides NMM, other dyes can also be incorporated into CPNs. Different dyes present distinct

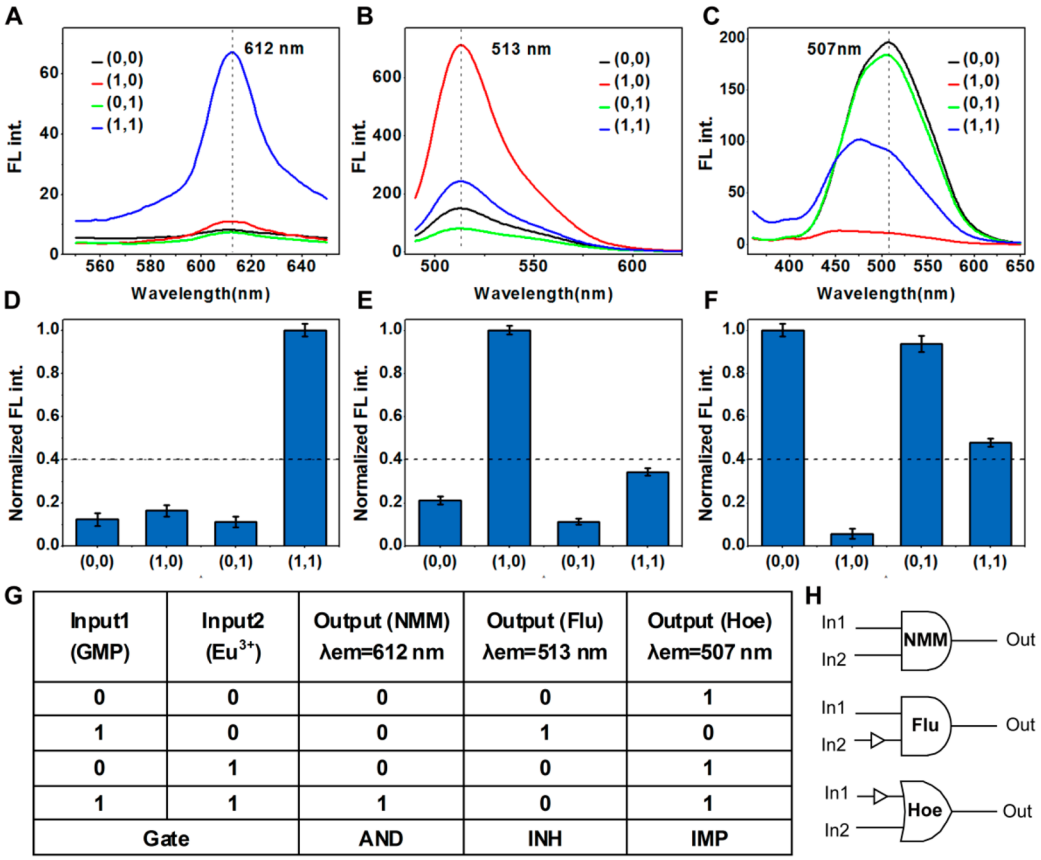

Input1 (GMP)	Input2 (Eu^{3+})	Output (NMM) λem=612 nm	Output (Flu) λem=513 nm	Output (Hoe) λem=507 nm
0	0	0	0	1
1	0	0	1	0
0	1	0	0	1
1	1	1	0	1
Gate		AND	INH	IMP

Figure 3. (A) Fluorescence spectra of NMM with different combinations of the inputs upon excitation at 399 nm. (B) Fluorescence spectra of fluorescein upon excitation at 485 nm. (C) Fluorescence spectra of Hoechst 33342 upon excitation at 352 nm. [GMP] = 0.5 mM, [Eu^{3+}] = 0.125 mM, [dye] = 0.2 μM. Histograms of normalized fluorescence intensities of (D) NMM at 612 nm, (E) fluorescein at 513 nm, and (F) Hoechst 33342 at 507 nm, corresponding to different logic gates. (G) Truth table and (H) logic schemes for the different logic gates.

fluorescence properties in the aqueous solution and in the presence of CPNs. Free NMM is nonfluorescent in aqueous solution, whereas its fluorescence can be enhanced upon encapsulation in the CPNs generated from GMP and Eu^{3+}. Individual GMP or Eu^{3+} has little effect on its emission, as shown in Figure 3A. NMM could be viewed as a gate and GMP and Eu^{3+} could act as two inputs. The absence and presence of these inputs was considered as 0 and 1, respectively. The relative fluorescence intensity of NMM at 612 nm could be regarded as the output with a threshold value of 0.4. The response pattern to inputs generated an AND gate (Figure 3D,G). Then we investigated the behaviors of other two fluorescent dyes before and after encapsulation. Fluorescein (Flu), whose structure is shown in Figure S5A (Supporting Information), is widely used as a fluorescent tracer for many applications. It has an emission maximum of 513 nm upon excitation at 485 nm (Figure 3B). It was found that the fluorescent intensity of Flu was greatly enhanced in the presence of GMP and quenched partly by Eu^{3+} ions. After adding GMP and Eu^{3+} simultaneously, weak fluorescence enhancement was observed. Although the mechanism of fluorescence switching of Flu is unclear up to now, we can still employ its properties to construct a logic gate. Flu could be regarded as a gate, while GMP and Eu^{3+} still acted as two inputs. The relative fluorescence intensity of Flu at 513 nm could be regarded as the output with a threshold value of 0.4. Free Flu and Flu/Eu^{3+} resulted in output value 0 and Flu/GMP gave rise to 1. Although the relative fluorescence intensity of Flu in the presence of GMP and Eu^{3+} was higher than that of free Flu, it was still lower than the threshold value, corresponding to output 0. An INH gate was constructed by observing the fluorescence at 513 nm in response to different combinations of inputs (Figure 3E,G). Hoechst 33342 (Hoe), whose structure is shown in Figure S5B (Supporting Information), is often used for staining nucleic acids and intracellular imaging. Hoe emits fluorescence around 510 nm in the absence of nucleic acid when excited by ultraviolet light at around 350 nm (Figure 3C). Different from NMM and Flu, the fluorescence of Hoe was quenched completely by GMP, whereas Eu^{3+} had little effect on its emission. However, the fluorescence was recovered partly when Hoe was confined in the CPNs of GMP and Eu^{3+}. Meanwhile, the emission peak shifted from 507 to 485 nm and the corresponding color changed from green to blue (Figures S6 and S7, Supporting Information). When Hoe served as a gate, its fluorescent response to input combinations of GMP and Eu^{3+} corresponded to an IMP gate (Figure 3F,G). The output value was 0 only when GMP was added. The above results demonstrated that three different logic gates were constructed using the different guest molecules and the same input combinations (Figure 3H). It implies that the dimension of molecular logic gates will be further extended by employing dyes with different fluorescent properties.

dx.doi.org/10.1021/am501949t | ACS Appl. Mater. Interfaces 2014, 6, 9557−9562

CONCLUSION

In summary, we used nucleotide, lanthanide ions, and NMM as building blocks to fabricate a system, whose behavior could be described by a variety of logic gates exhibiting fluorescence emission as the optical output in response to the inputs. The logic system presented here demonstrated the first example of "plug and play logic gate based on nucleotide, in which the addition of new modules directly enabled new logic functions. PASS 0, YES, PASS 1, NOT, IMP, OR, and AND gates were successfully constructed in sequence. Furthermore, by changing the dyes, AND, INH, and IMP gates were fabricated. It is very simple in design and different logic gates can be self-assembled from components that are mixed in aqueous solution. Additionally, detection of output signals is convenient using fluorescence spectroscopy and sophisticated equipment are not required. Our material shows the potential for bioapplications, such as bioimaging, pH sensor, and pH-sensitive drug release owing to fluorescence property and pH-sensitivity of CPNs, and photodynamic activity of NMM. Although there is still much work to do in the field, this proof-of-concept could provide a general route to the design of various biomolecule-based logic systems.

ASSOCIATED CONTENT

Supporting Information

SEM images of the CPNs. Chemical structures of dyes used. Fluorescence spectra of various logic gates in response to different combinations of inputs. This material is available free of charge via the Internet at http://pubs.acs.org.

AUTHOR INFORMATION

Corresponding Authors

*J. Ren. Email: jren@ciac.ac.cn.
*X. Qu. Email: xqu@ciac.ac.cn.

Notes

The authors declare no competing financial interest.

ACKNOWLEDGMENTS

Financial support was provided by the National Basic Research Program of China (2012CB720602 and 2011CB936004) and the National Natural Science Foundation of China (91213302, 21210002, and 21303182).

REFERENCES

(1) de Silva, A. P.; Gunaratne, H. Q. N.; Mccoy, C. P. A Molecular Photoionic and Gate Based on Fluorescent Signaling. *Nature* **1993**, *364*, 42−44.
(2) Raymo, F. M. Digital Processing and Communication with Molecular Switches. *Adv. Mater.* **2002**, *14*, 401−414.
(3) de Silva, A. P.; McClenaghan, N. D. Molecular-Scale Logic Gates. *Chem.—Eur. J.* **2004**, *10*, 574−586.
(4) Andreasson, J.; Pischel, U. Smart Molecules at Work-Mimicking Advanced Logic Operations. *Chem. Soc. Rev.* **2010**, *39*, 174−188.
(5) Katz, E.; Privman, V. Enzyme-Based Logic Systems for Information Processing. *Chem. Soc. Rev.* **2010**, *39*, 1835−1857.
(6) de Silva, A. P. Molecular Logic Gate Arrays. *Chem.—Asian J.* **2011**, *6*, 750−766.
(7) Wu, Y.; Xie, Y.; Zhang, Q.; Tian, H.; Zhu, W.; Li, A. D. Q. Quantitative Photoswitching in Bis(dithiazole)ethene Enables Modulation of Light for Encoding Optical Signals. *Angew. Chem., Int. Ed.* **2014**, *53*, 2090−2094.
(8) Chen, S.; Yang, Y.; Wu, Y.; Tian, H.; Zhu, W. Multi-Addressable Photochromic Terarylene Containing Benzo[*b*]thiophene-1,1-dioxide Unit as Ethene Bridge: Multifunctional Molecular Logic Gates on Unimolecular Platform. *J. Mater. Chem.* **2012**, *22*, 5486−5494.
(9) Chen, S.; Guo, Z.; Zhu, S.; Shi, W. E.; Zhu, W. A Multiaddressable Photochromic Bisthienylethene with Sequence-Dependent Responses: Construction of an Inhibit Logic Gate and a Keypad Lock. *ACS Appl. Mater. Interfaces* **2013**, *5*, 5623−5629.
(10) Pu, F.; Ren, J.; Yang, X.; Qu, X. Multivalued Logic Gates Based on DNA. *Chem.—Eur. J.* **2011**, *17*, 9590−9594.
(11) Bavireddi, H.; Bharate, P.; Kikkeri, R. Use of Boolean and Fuzzy Logics in Lactose Glycocluster Research. *Chem. Commun.* **2013**, *49*, 9185−9187.
(12) de Silva, A. P.; Dobbin, C. M.; Vance, T. P.; Wannalerse, B. Multiply Reconfigurable 'Plug and Play' Molecular Logic *via* Self-Assembly. *Chem. Commun.* **2009**, 1386−1388.
(13) Pei, H.; Liang, L.; Yao, G.; Li, J.; Huang, Q.; Fan, C. Reconfigurable Three-Dimensional DNA Nanostructures for the Construction of Intracellular Logic Sensors. *Angew. Chem., Int. Ed.* **2012**, *51*, 9020−9024.
(14) Miyoshi, D.; Inoue, M.; Sugimoto, N. DNA Logic Gates Based on Structural Polymorphism of Telomere DNA Molecules Responding to Chemical Input Signals. *Angew. Chem., Int. Ed.* **2006**, *45*, 7716−7719.
(15) Macdonald, J.; Li, Y.; Sutovic, M.; Lederman, H.; Pendri, K.; Lu, W.; Andrews, B. L.; Stefanovic, D.; Stojanovic, M. N. Medium Scale Integration of Molecular Logic Gates in an Automaton. *Nano Lett.* **2006**, *6*, 2598−2603.
(16) Chen, X.; Wang, Y.; Liu, Q.; Zhang, Z.; Fan, C.; He, L. Construction of Molecular Logic Gates with a DNA-Cleaving Deoxyribozyme. *Angew. Chem., Int. Ed.* **2006**, *45*, 1759−1762.
(17) Gianneschi, N. C.; Ghadiri, M. R. Design of Molecular Logic Devices Based on a Programmable DNA-Regulated Semisynthetic Enzyme. *Angew. Chem., Int. Ed.* **2007**, *46*, 3955−3958.
(18) Elbaz, J.; Moshe, M.; Willner, I. Coherent Activation of DNA Tweezers: A "SET-RESET" Logic System. *Angew. Chem., Int. Ed.* **2009**, *48*, 3834−3837.
(19) Feng, X.; Duan, X.; Liu, L.; Feng, F.; Wang, S.; Li, Y.; Zhu, D. Fluorescence Logic-Signal-Based Multiplex Detection of Nucleases with the Assembly of a Cationic Conjugated Polymer and Branched DNA. *Angew. Chem., Int. Ed.* **2009**, *48*, 5316−5321.
(20) Bi, S.; Yan, Y.; Hao, S.; Zhang, S. Colorimetric Logic Gates Based on Supramolecular DNAzyme Structures. *Angew. Chem., Int. Ed.* **2010**, *49*, 4438−4442.
(21) Pu, F.; Wang, C.; Hu, D.; Huang, Z.; Ren, J.; Wang, S.; Qu, X. Logic Gates and pH Sensing Devices Based on a Supramolecular Telomere DNA/Conjugated Polymer System. *Mol. BioSyst.* **2010**, *6*, 1928−1932.
(22) Wen, Y.; Xu, L.; Li, C.; Du, H.; Chen, L.; Su, B.; Zhang, Z.; Zhang, X.; Song, Y. DNA-Based Intelligent Logic Controlled Release Systems. *Chem. Commun.* **2012**, *48*, 8410−8412.
(23) Cornett, E. M.; Campbell, E. A.; Gulenay, G.; Peterson, E.; Bhaskar, N.; Kolpashchikov, D. M. Molecular Logic Gates for DNA Analysis: Detection of Rifampin Resistance in M. Tuberculosis DNA. *Angew. Chem., Int. Ed.* **2012**, *51*, 9075−9077.
(24) Kalia, D.; Merey, G.; Nakayama, S.; Zheng, Y.; Zhou, J.; Luo, Y.; Guo, M.; Roembke, B. T.; Sintim, H. O. Nucleotide, c-di-GMP, c-di-AMP, cGMP, cAMP, (p)ppGpp Signaling in Bacteria and Implications in Pathogenesis. *Chem. Soc. Rev.* **2013**, *42*, 305−341.
(25) Dooley, C. J.; Rouge, J.; Ma, N.; Invernale, M.; Kelley, S. O. Nucleotide-Stabilized Cadmium Sulfide Nanoparticles. *J. Mater. Chem.* **2007**, *17*, 1687−1691.
(26) Kumar, A.; Kumar, V. Synthesis and Optical Properties of Guanosine 5′-Monophosphate-Mediated Cds Nanostructures: An Analysis of Their Structure, Morphology, and Electronic Properties. *Inorg. Chem.* **2009**, *48*, 11032−11037.
(27) Li, M.; Oakley, R. J.; Bevan, H.; Smarsly, B. M.; Mann, S.; Faul, C. F. J. Nucleotide-Based Templates for Nanoparticle Production—Exploiting Multiple Noncovalent Interactions. *Chem. Mater.* **2009**, *21*, 3270−3274.

(28) Pandoli, O.; Massi, A.; Cavazzini, A.; Spada, G. P.; Cui, D. Circular Dichroism and UV-Vis Absorption Spectroscopic Monitoring of Production of Chiral Silver Nanoparticles Templated by Guanosine 5′-Monophosphate. *Analyst* **2011**, *136*, 3713−3719.
(29) Huang, P.; Pandoli, O.; Wang, X.; Wang, Z.; Li, Z.; Zhang, C.; Chen, F.; Lin, J.; Cui, D.; Chen, X. Chiral Guanosine 5′-Monophosphate-Capped Gold Nanoflowers: Controllable Synthesis, Characterization, Surface-Enhanced Raman Scattering Activity, Cellular Imaging and Photothermal Therapy. *Nano Res.* **2012**, *5*, 630−639.
(30) Aime, C.; Nishiyabu, R.; Gondo, R.; Kaneko, K.; Kimizuka, N. Controlled Self-Assembly of Nucleotide-Lanthanide Complexes: Specific Formation of Nanofibers from Dimeric Guanine Nucleotides. *Chem. Commun.* **2008**, 6534−6536.
(31) Nishiyabu, R.; Aime, C.; Gondo, R.; Noguchi, T.; Kimizuka, N. Confining Molecules within Aqueous Coordination Nanoparticles by Adaptive Molecular Self-Assembly. *Angew. Chem., Int. Ed.* **2009**, *48*, 9465−9468.
(32) Nishiyabu, R.; Hashimoto, N.; Cho, T.; Watanabe, K.; Yasunaga, T.; Endo, A.; Kaneko, K.; Niidome, T.; Murata, M.; Adachi, C.; Katayama, Y.; Hashizume, M.; Kimizuka, N. Nanoparticles of Adaptive Supramolecular Networks Self-Assembled from Nucleotides and Lanthanide Ions. *J. Am. Chem. Soc.* **2009**, *131*, 2151−2158.
(33) Nishiyabu, R.; Aime, C.; Gondo, R.; Kaneko, K.; Kimizuka, N. Selective Inclusion of Anionic Quantum Dots in Coordination Network Shells of Nucleotides and Lanthanide Ions. *Chem. Commun.* **2010**, *46*, 4333−4335.
(34) Hu, D.; Ren, J.; Qu, X. Metal-Mediated Fabrication of New Functional G-Quartet-Based Supramolecular Nanostructure and Potential Application as Controlled Drug Release System. *Chem. Sci.* **2011**, *2*, 1356−1361.
(35) Dash, J.; Patil, A. J.; Das, R. N.; Dowdall, F. L.; Mann, S. Supramolecular Hydrogels Derived from Silver Ion-Mediated Self-Assembly of 5′-Guanosine Monophosphate. *Soft Matter* **2011**, *7*, 8120−8126.
(36) Lopez, A.; Liu, J. Light-Activated Metal-Coordinated Supramolecular Complexes with Charge-Directed Self-Assembly. *J. Phys. Chem. C* **2013**, *117*, 3653−3661.
(37) Qi, C.; Zhu, Y. J.; Zhao, X. Y.; Lu, B. Q.; Tang, Q. L.; Zhao, J.; Chen, F. Highly Stable Amorphous Calcium Phosphate Porous Nanospheres: Microwave-Assisted Rapid Synthesis Using Atp as Phosphorus Source and Stabilizer, and Their Application in Anticancer Drug Delivery. *Chem.—Eur. J.* **2013**, *19*, 981−987.
(38) Baytekin, H. T.; Akkaya, E. U. A Molecular NAND Gate Based on Watson-Crick Base Pairing. *Org. Lett.* **2000**, *2*, 1725−1727.
(39) de Sousa, M.; Kluciar, M.; Abad, S.; Miranda, M. A.; de Castro, B.; Pischel, U. An Inhibit (INH) Molecular Logic Gate Based on 1,8-Naphthalimide-Sensitised Europium Luminescence. *Photochem. Photobiol. Sci.* **2004**, *3*, 639−642.
(40) Claussen, J. C.; Algar, W. R.; Hildebrandt, N.; Susumu, K.; Ancona, M. G.; Medintz, I. L. Biophotonic Logic Devices Based on Quantum Dots and Temporally-Staggered Forster Energy Transfer Relays. *Nanoscale* **2013**, *5*, 12156−12170.
(41) Claussen, J. C.; Hildebrandt, N.; Susumu, K.; Ancona, M. G.; Medintz, I. L. Complex Logic Functions Implemented with Quantum Dot Bionanophotonic Circuits. *ACS Appl. Mater. Interfaces* **2014**, *6*, 3771−3778.
(42) Pu, F.; Ju, E.; Ren, J.; Qu, X. Multiconfigurable Logic Gates Based on Fluorescence Switching in Adaptive Coordination Polymer Nanoparticles. *Adv. Mater.* **2014**, *26*, 1111−1117.
(43) Xing, L.; Zheng, H.; Che, S. A pH-Responsive Cleavage Route Based on a Metal-Organic Coordination Bond. *Chem.—Eur. J.* **2011**, *17*, 7271−7275.
(44) Gao, P. F.; Zheng, L. L.; Liang, L. J.; Yang, X. X.; Li, Y. F.; Huang, C. Z. A New Type of pH-Responsive Coordination Polymer Sphere as a Vehicle for Targeted Anticancer Drug Delivery and Sustained Release. *J. Mater. Chem. B* **2013**, *1*, 3202−3208.